Optik 157 (2018) 1259–1266

Contents lists available at ScienceDirect

Optik

journal homepage: www.elsevier.de/ijleo

Spectrum reconstruction for five-channel autocorrelation function of spectropolarimeter

Jirui Zhang, Chunmin Zhang*, Tingyu Yan, Zeyu Chen

Institute of Space Optics, School of Science, Xi'an Jiaotong University, Xi'an, 710049, China

ARTICLE INFO

Article history:
Received 19 July 2017
Accepted 14 December 2017

Keywords:
Spectropolarimeter
The ratio of retarder
Five-channel
Spectrum reconstruction

ABSTRACT

The effect of the ratio of two retarders for the demodulation in the intensity modulation spectropolarimeter is proposed. The five-channel autocorrelation function is introduced for the first time, its forming conditions and the principle of spectrum reconstruction are analyzed. From the analysis of the spectropolarimeter based on the interference spectrometer, we can conclude that the spectral resolution of some Stokes parameters reconstructed by the five-channel interferogram is improved compared with the seven-channel interferogram. The simulation experiment of spectrum recovery of five-channel autocorrelation function is carried out. The simulation results are in good agreement with the theory, and the results show that the scheme of the five-channel is feasible, which provides a good theoretical basis and reference for the optimization design of the spectropolarimeter.

1. Introduction

Spectral and polarization information can be used to analyze and identify the target [1]. Spectral analysis can obtain the target component information [2], and the surface structure and edge features of the target can be known by the polarization information [3–5], and polarization information of light can be completely described by Stokes vector [6–8]. The intensity modulation spectropolarimeter is the combination of these two technologies together to achieve the simultaneous detection of spectral and polarization information [9].

The intensity modulation spectropolarimeter was first described by Oka and Kato in 1999 [10]. The design has the advantage of compact structure, and no moving parts, can quickly obtain the target spectral information and polarization information [11]. The main components of the spectropolarimeter are composed of two parts: the polarization modulation part and the spectrometer part, when a beam of light passes through a polarization modulation part, four Stokes parameters of light can be modulated at different frequencies of the carrier signal, which forms a linear superposition of power spectrum, the spectrometer and detector will detect the power spectrum and then transmit the detected signals to the computer [9,12]. Finally, Stokes vector and spectrum information of target can be obtained by computer.

Since the polarization modulation section is the key part of spectropolarimeter for spectrum recovery, we focus on the polarization modulation part. The five-channel autocorrelation function and the principle of spectrum reconstruction of five-channel autocorrelation function of spectropolarimeter is described in Section 2. Section 3 gives the simulation experiment of spectral reconstruction and presents the advantage of five-channel interferogram. The simulation result is discussed and conclusion is contained in Section 4.

* Corresponding author.
E-mail address: zcm@mail.xjtu.edu.cn (C. Zhang).

https://doi.org/10.1016/j.ijleo.2017.12.067
0030-4026/

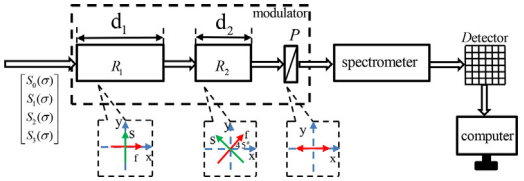

Fig. 1. The optical layout of the spectropolarimeter.

2. Five-channel autocorrelation function of spectropolarimeter

2.1. The modulation principle of spectropolarimeter

The optical layout of the spectropolarimeter is depicted Fig. 1. It can be seen from the figure that the components of the spectropolarimeter are modulator, spectrometer, detector and computer. The modulator section is composed of two retarders R_1, R_2 and a polarizer P, the fast aexs of R_1 is aligned with the transmission axes of P at an angle of 45^o relative to the fast aexs of R_2.

When the light passes through the polarization modulation section, four Stokes parameters of light can be modulated at different frequencies of the carrier signal. According to the theory of polarization optics, the modulated Stokes vector can be expressed in the following form [13]:

$$\begin{bmatrix} s_0'(\sigma) \\ s_1'(\sigma) \\ s_2'(\sigma) \\ s_3'(\sigma) \end{bmatrix} = \begin{bmatrix} ½ & ½ & 0 & 0 \\ ½ & ½ & 0 & 0 \\ 0 & 0 & 0 & 0 \\ 0 & 0 & 0 & 0 \end{bmatrix} \begin{bmatrix} 1 & 0 & 0 & 0 \\ 0 & \cos\varphi_2(\sigma) & 0 & -\sin\varphi_2(\sigma) \\ 0 & 0 & 0 & 0 \\ 0 & \sin\varphi_2(\sigma) & 0 & \cos\varphi_2(\sigma) \end{bmatrix} \cdot \begin{bmatrix} 1 & 0 & 0 & 0 \\ 0 & 1 & 0 & 0 \\ 0 & 0 & \cos\varphi_1(\sigma) & \sin\varphi_1(\sigma) \\ 0 & 0 & \sin\varphi_1(\sigma) & \cos\varphi_1(\sigma) \end{bmatrix} \begin{bmatrix} s_0(\sigma) \\ s_1(\sigma) \\ s_2(\sigma) \\ s_3(\sigma) \end{bmatrix} \tag{1}$$

Where the right side of the equation is the Mueller matrix of polarizer, retarder R_2 and R_1, and the Stokes vector of the incident light, $\varphi_1(\sigma)$ and $\varphi_2(\sigma)$are the phase retardations of R_1 and R_2,$\varphi_j = 2\pi\Delta n d_j\sigma(j = 1, 2)$, σ is wave number, d_j is the thickness of R_1 and R_2 and Δn is the birefringence of the birefringent crystal. S_0 is the total intensity of the light, S_1 is the difference between linear polarizations of 0° and 90°, S_2 is the difference between linear polarizations of $\pm 45^\circ$, and S_3 is the difference between right and left circular polarization [11]. Because the digital camera is just responding to radiation intensity instead of polarization state [14], only $s_0'(\sigma)$ can be measured. $s_0'(\sigma)$can be expressed as [10]:

$$P(\sigma) = (1/2)S_0(\sigma) + (1/2)S_1(\sigma)\cos[\varphi_2(\sigma)] + (1/2)S_2(\sigma)\sin[\varphi_2(\sigma)]\sin[\varphi_1(\sigma)] - (1/2)S_3(\sigma)\sin[\varphi_2(\sigma)]\cos[\varphi_1(\sigma)] \tag{2}$$

The Stokes vector can be obtained by demodulating the autocorrelation function, Fourier transform demodulation is a good choice for demodulation [15]. Eq. (2) can be rearranged into

$$\begin{aligned} P(\sigma) &= (1/2)S_0(\sigma) + (1/4)S_1(\sigma)(e^{i2\pi L_2\sigma} + e^{-i2\pi L_2\sigma}) + (1/8)\left[S_{23}(\sigma)e^{i2\pi(L_1-L_2)\sigma} + S_{23}^*(\sigma)e^{-i2\pi(L_1-L_2)\sigma}\right] \\ &-(1/8)\left[S_{23}(\sigma)e^{i2\pi(L_1+L_2)\sigma} + S_{23}^*(\sigma)e^{-i2\pi(L_1+L_2)\sigma}\right] \end{aligned} \tag{3}$$

With

$$S_{23}(\sigma) = S_2(\sigma) - iS_3(\sigma) \tag{4}$$

where L_j is the optical path difference of R_1 and R_2, $L_j = \Delta n d_j$(j = 1,2), Δn is almost constant for the general crystal, so the optical path difference mainly depends on the thickness of the retarder. It can be seen from Eq. (3) that each Stokes parameter is modulated on seven different frequency components, respectively are0, $\pm\varphi_2$, $\pm[\varphi_1 - \varphi_2]$, $\pm[\varphi_1 + \varphi_2]$, the center frequency of each carrier signal is determined by these.

The autocorrelation function is the Fourier inverse transform of Eq. (3):

$$\begin{aligned} C(h) &= (1/2)A_0(h) + (1/4)A_1(h - L_2) + (1/4)A_1^*(-h - L_2) + (1/8)A_2[h - (L_1 - L_2)] \\ &+(1/8)A_2^*[-h - (L_1 - L_2)] - (1/8)A_3[h - (L_1 + L_2)] - (1/8)A_3^*[-h - (L_1 + L_2)] \\ &= C_0 + C_{-1} + C_1 + C_{-2} + C_2 - C_{-3} - C_3 \end{aligned} \tag{5}$$

Table 1
The number of channels for different thickness ratio of two retarders.

$L_1 : L_2$	h							
	$-(L_1+L_2)$	$-L_2$	$-(L_1-L_2)$	0	L_1-L_2	L_2	L_1+L_2	The number of channels
1:2	$-3L_1$	$-2L_1$	L_1	0	$-L_1$	$2L_1$	$3L_1$	7
1:1	$-2L_2$	$-L_2$	0	0	0	L_2	$2L_2$	5
2:1	$-3L_2$	$-L_2$	$-L_2$	0	L_2	L_2	$3L_2$	5

where

$$A_0(h) = \mathrm{F}^{-1}\left[S_0(\sigma)\right] \tag{6a}$$

$$A_1(h) = \mathrm{F}^{-1}\left[S_1(\sigma)\right] \tag{6b}$$

$$A_2(h) = \mathrm{F}^{-1}\left[S_{23}^*(\sigma)\right] \tag{6c}$$

$$A_3(h) = \mathrm{F}^{-1}\left[S_{23}^*(\sigma)\right] \tag{6d}$$

where h represents the different optical path difference, $\mathrm{F}^{-1}$is Fourier inverse transform. Eq. (5) is composed of seven items. From Eqs. (5) and (6a)–(6d) we can see that the first item contains$S_0(\sigma)$, the second and third item contain$S_1(\sigma)$, and the remaining four items all contain $S_2(\sigma)$and$S_3(\sigma)$. These seven items are selected by filtering, and then four Stokes parameters can be demodulated from Eq. (7a)–(7c).

$$F_1(\sigma) = (1/2)S_0(\sigma) \tag{7a}$$

$$F_2(\sigma) = (1/4)S_1(\sigma)\exp(-i\phi_2(\sigma)) \tag{7b}$$

$$F_3(\sigma) = (1/8)\left[S_2(\sigma) - iS_3(\sigma)\right]\exp\left\{i\left[\phi_1(\sigma) - \phi_2(\sigma)\right]\right\} \tag{7c}$$

2.2. The spectrum reconstruction of five-channel autocorrelation function

It can be seen from Eq. (5) that the autocorrelation function has seven optical path difference channels, and the different channels can be used to reconstruct each Stokes parameter. The previous theory only considers the situation in which the seven channels are separated from each other, we find that the number of channels becomes five in some special conditions. Although some channels overlap, the Stokes vector can still be reconstructed. As can be seen from Table 1, when the thickness ratio of the two retarders is 1:1 or 2:1, the number of channels reduced to five. We choose the ratio of 2:1 for detailed description, optical path difference of $L_1 - L_2$ and L_2 of the two channels overlap, and optical path difference of $-(L_1 - L_2)$ and $-L_2$ of the two channels overlap, meaning that the item contains the $S_1(\sigma)$ information and containing $S_2(\sigma)$, $S_3(\sigma)$ information overlap with each other, so the autocorrelation function only contains five channels. There are other channels containing$S_2(\sigma)$, $S_3(\sigma)$ without overlapping with others, which just makes it difficult to reconstruct the$S_1(\sigma)$, but the $S_1(\sigma)$ can be demodulated by using some mathematical transformation.

At this time, Eq. (5) becomes:

$$\begin{aligned} C(h) &= (1/2)A_0(h) + (1/4)A_1(h - L_2) + (1/4)A_1^*(-h - L_2) \\ &-(1/8)A_3\left[h - (L_1 + L_2)\right] - (1/8)A_3^*\left[-h - (L_1 + L_2)\right] \\ &= \mathrm{C}_0 + \mathrm{C}_{-1} + \mathrm{C}_1 - \mathrm{C}_{-3} - \mathrm{C}_3 \end{aligned} \tag{8}$$

where

$$A_0(h) = \mathrm{F}^{-1}\left[S_0(\sigma)\right] \tag{9a}$$

$$A_1(h) = \mathrm{F}^{-1}\left[S_1(\sigma) + (1/2)S_{23}^*(\sigma)\right] \tag{9b}$$

$$A_3(h) = \mathrm{F}^{-1}\left[S_{23}^*(\sigma)\right] \tag{9c}$$

We choose the first and the forth items of Eq. (8) to demodulate$S_0(\sigma)$, $S_2(\sigma)$and $S_3(\sigma)$.

$$F_0(\sigma) = (1/2)S_0(\sigma) \tag{10a}$$

$$F_3(\sigma) = (1/8)\left[S_2(\sigma) + iS_3(\sigma)\right]\exp\left\{-i\left[\phi_1(\sigma) + \phi_2(\sigma)\right]\right\} \tag{10b}$$

After getting $S_2(\sigma)$ and $S_3(\sigma)$, the Fourier transform of the second item of Eq. (8) can be used to demodulate $S_1(\sigma)$.

$$F_1(\sigma) = (1/4)[S_1(\sigma) + (1/2)S_{23}^*(\sigma)] \tag{11}$$

$$S_1(\sigma) = 4 * F_1(\sigma) - (1/2)S_{23}^*(\sigma) \tag{12}$$

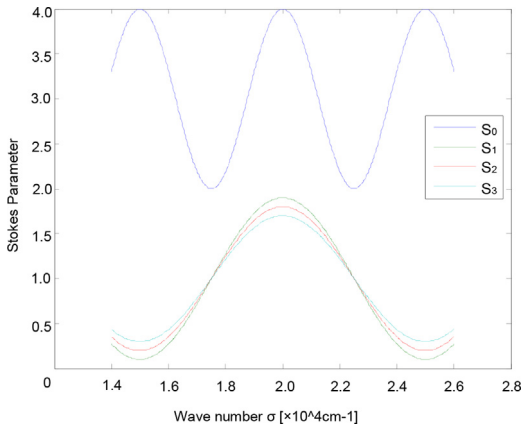

Fig. 2. Input Stokes Spectrum.

The principle of spectrum reconstruction of five-channel autocorrelation function is obtained now. For the ratio of 1:1 of two retarders, we can get the reconstruction spectrum by the same mathematical method. It is important to note that when the ratio is 1:1, the three channels with the optical path difference of $-(L_1 - L_2)$, 0 and $L_1 - L_2$ completely overlap.

3. The simulation experiment of spectrum reconstruction of five-channel autocorrelation function and the advantage of five-channel interferogram

3.1. The simulation experiment of spectrum reconstruction

We assume that the input spectral range is $1.4 \times 10^4 \mathrm{cm}^{-1}(714nm) \sim 2.6 \times 10^4 \mathrm{cm}^{-1}(385nm)$, and the retarder material is quartz, its birefringence Δn is approximate 0.01. For seven-channel, the thickness of R_1 and R_2 are 0.6 cm and 1.2 cm, respectively. For the five-channel, the ratio is 1:1, the thickness of R_1 and R_2 both are 0.6 cm, and when the ratio is 2:1, the thickness are 1.2 cm and 0.6 cm. The spectra of the four Stokes vectors of the simulated input light are shown in Fig. 2.

There are different modulation spectrums for different thickness ratio of two retarders. Fig. 3 shows that the different modulation spectrum and autocorrelation function for different ratio of two retarders.

It can be seen from Fig. 3(b*) and (c*) that although both of them are five-channel autocorrelation function, the optical path difference of each channel is different with each other, so the channel selection for spectrum reconstruction is different. The retarder ratio of 2:1 of five-channel autocorrelation function is chosen to describe the spectrum reconstruction process. According to Eq. (10a) and (10b), we select the two channels with the optical path difference of 0 and $L_1 + L_2$ to reconstruct spectrum, we can get the spectrum of $S_0(\sigma)$, $S_2(\sigma)$ and $S_3(\sigma)$, and then the optical path difference channel of L_2 is demodulated, combined with Eq. (12), the spectrum of $S_1(\sigma)$ can be obtained. Fig. 4 is the Stokes vector spectrum we obtained by the above method.

Fig. 4 shows the spectrum of the four Stokes parameters, which is obtained when the ratio of the two retarders is 2:1, and it can be seen that the reconstructed spectrum coincide well with the original spectra, which indicates that the method of five-channel autocorrelation function is feasible for the spectrum reconstruction. For the ratio of 1:1, the Stokes vector spectrum can also be obtained in a similar way, except that the channel selection is somewhat different from the ratio of 2:1.

3.2. The advantage of five-channel interferogram

We now analyze the spectropolarimeter based on the interference spectrometer. After the incident light passes through the modulator and the interference spectrometer, the expression of the intensity of the light detected on the detector as follow:

$$\mathrm{I} \propto \int \frac{(1+\cos\varphi)}{2} \left\{ \mathrm{S}_0(\sigma) + \mathrm{S}_1(\sigma)\cos\left[\varphi_2(\sigma)\right] + \mathrm{S}_2(\sigma)\sin\left[\varphi_2(\sigma)\right]\sin\left[\varphi_1(\sigma)\right] - \mathrm{S}_3(\sigma)\sin\left[\varphi_2(\sigma)\right]\cos\left[\varphi_1(\sigma)\right] \right\} d\sigma \tag{12}$$

φ is the phase difference produced by the light through the interference spectrometer. Fig. 5 is the interferogram for the ratio of two retarders of 2:1 and 1:2, the red curve is seven-channel interferogram and the green curve is five-channel

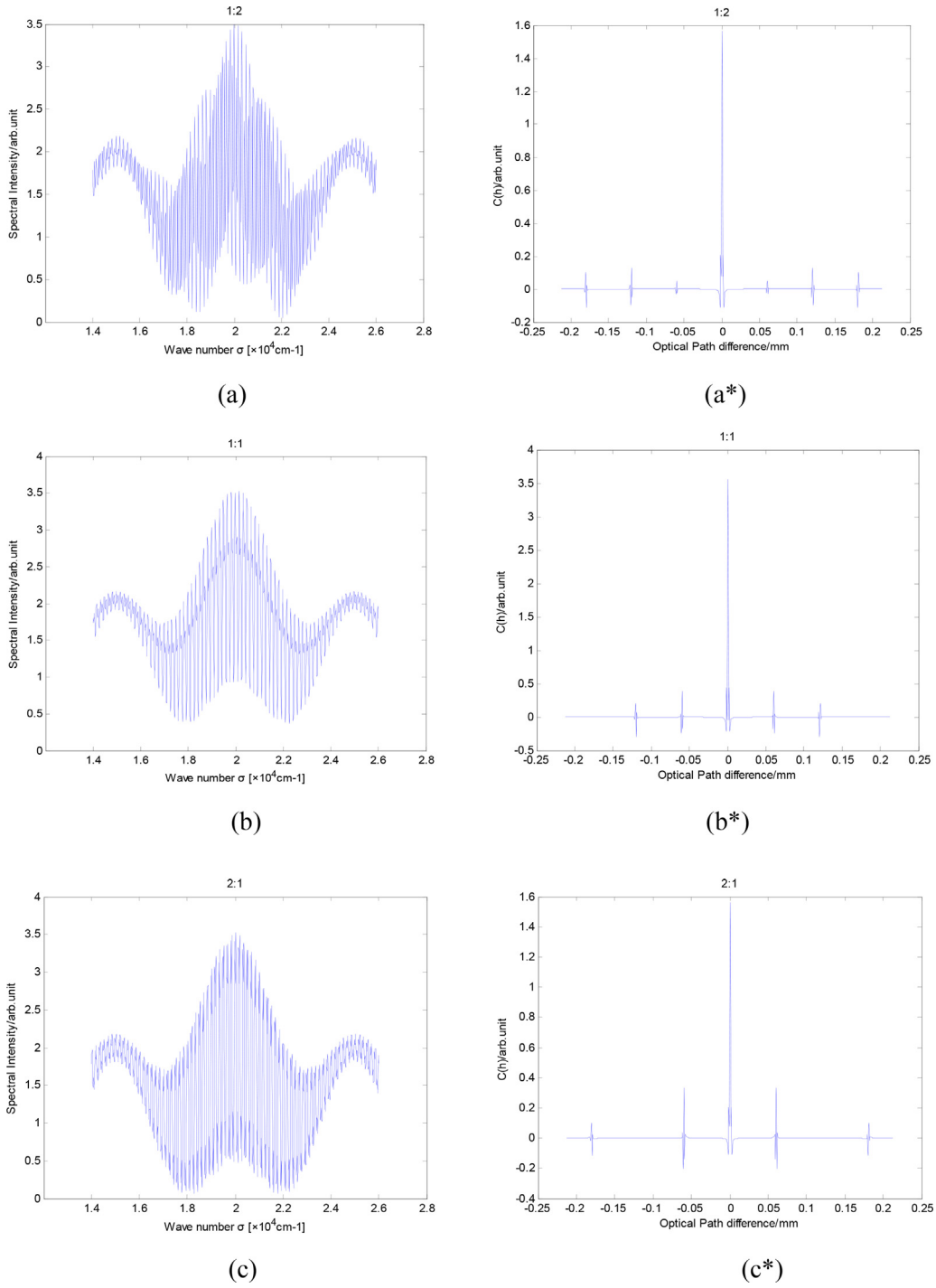

Fig. 3. The different modulation spectrum (a–c) and autocorrelation function (a*–c*) corresponding to different retarder ratios.

interferogram. It can be seen from Fig. 5 that the maximum optical path difference of one-side sampling for each channel of seven-channel interferogram as follow:

$$\Delta_{7s} = \frac{\Delta_{\max}}{7} \tag{13}$$

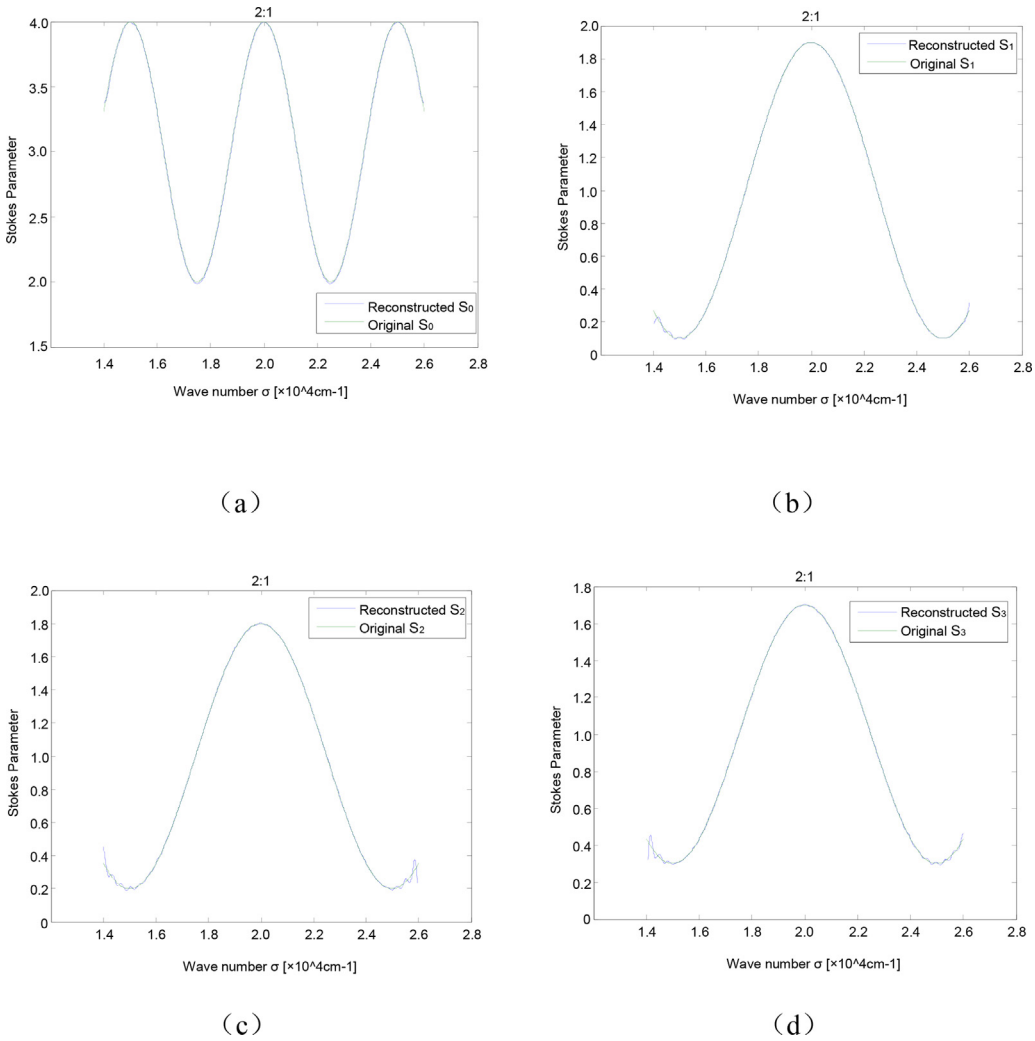

Fig. 4. The original spectrum and reconstruction spectrum of four Stokes parameters.

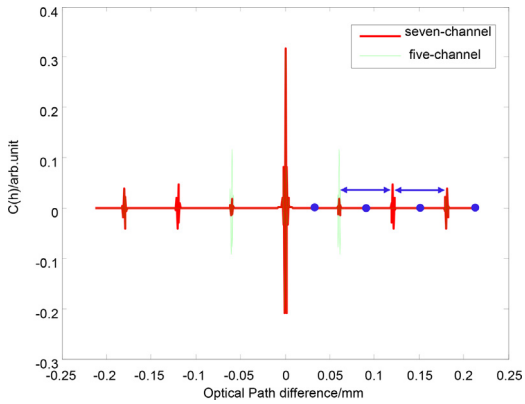

Fig. 5. The interferogram of retarder ratio of 2:1 and 1:2. (For interpretation of the references to colour in this figure legend, the reader is referred to the web version of this article.)

$\Delta_{\max}$ is the maximum optical path difference of the spectropolarimeter. The spectral resolution of the reconstructed spectrum of each channel has the following relation to the one-side maximum optical path difference:

$$\delta\sigma_7 = \frac{1}{2\Delta_{7s}} = \frac{7}{2\Delta_{\max}} \tag{14}$$

For five-channel interferogram, the two channels with optical path difference of $L_1 - L_2$ and L_2 overlap, and the two channels with optical path difference of $-(L_1 - L_2)$ and $-L_2$ overlap. There is no channel at the optical path difference of $2L_2$and $-2L_2$, so the one-side maximum optical path difference (as indicated by the blue arrow in Fig. 5) of the two channels with the optical path difference of L_2 and $L_1 + L_2$can be expressed as:

$$\Delta_{5s} = \frac{2\Delta_{\max}}{7} \tag{15}$$

The spectral resolution of the reconstructed spectrum of the two channels is:

$$\delta\sigma_5 = \frac{1}{2\Delta_{5s}} = \frac{7}{4\Delta_{\max}} \tag{16}$$

It is meaning that the spectral resolution of S_1, S_2 and S_3 reconstructed by the five-channel interferogram is $7/4\Delta_{\max}$, this shows that the spectral resolution of S_1, S_2 and S_3 for the recovery spectrum of the five-channel interferogram is improved compared with the recovery spectrum of the seven-channel interferogram:

$$m = \frac{\delta\sigma_7}{\delta\sigma_5} = 2 \tag{17}$$

The same method can be used to obtain that the spectral resolution of S_2 and S_3 in the reconstructed spectrum is also improved by 3 times for the retarder thickness ratio of 1: 1.

4. Conclusion

The concept of five-channel autocorrelation function is proposed in this paper, and we can realize the five-channel autocorrelation function when the ratio of the two retarders is 1:1 and 2: 1, and the principle and method of its spectrum reconstruction are discussed in detail. A complete formula for spectral modulation and spectrum reconstruction is obtained. From the analysis of the spectropolarimeter based on the interference spectrometer, we can conclude that the spectral resolution of some Stokes parameters reconstructed by the five-channel interferogram is improved compared with the seven-channel interferogram, when the ratio is 2:1, the spectral resolution of S_1, S_2 and S_3 is increased by 2 times, and the spectral resolution of S_2 and S_3 is increased by a factor of 3 when the ratio is 1:1. The spectral reconstruction of the five-channel autocorrelation function with the ratio of 2:1 is simulated, the simulation results are consistent with our theoretical analysis, and the results show that the five-channel method is feasible, which provides a good theoretical reference for the optimization design of the higher resolution spectropolarimeter.

Acknowledgments

The work was supported by the Major Program of the National Natural Science Foundation of China (Grant No. 41530422), the National High Technology Research and Development Program of China (Grant No. 2012AA121101), the National Science and Technology Major Project of the Ministry of Science and Technology of China (Grant No. 32-Y30B08-9001-13/15), and the National Natural Science Foundation of China (Grant No. 61275184, 61540018, 61405153).

References

[1] D. Sabatke, A. Locke, E.L. Dereniak, M. Descour, J. Garcia, T. Hamilton, R.W. McMillan, Snapshot imaging spectropolarimeter, Opt. Eng. 41 (5) (2002) 1048–1054.
[2] R.G. Sellar, G.D. Boreman, Classification of imaging spectrometers for remote sensing applications, Opt. Eng. 44 (1) (2004), 13602.
[3] J.S. Tyo, D.L. Goldstein, D.B. Chenault, J.A. Shaw, Review of passive imaging polarimetry for remote sensing applications, Appl. Opt. 45 (22) (2006) 5453–5469.
[4] X.B. Sun, J. Hong, Y.L. Qiao, W.F. Yang, R.Z. Luo, Analysis of characteristic of multiband aerial polarization image, in: G.G. Matvienko (Ed.), SPIE-INT SOC OPTICAL ENGINEERING, BELLINGHAM PROCEEDINGS OF THE SOCIETY OF PHOTO-OPTICAL INSTRUMENTATION ENGINEERS(SPIE) vol. 5832 (2005) 219–227.
[5] F.J. Iannarilli, S.H. Jones, H.E. Scott, P.L. Kebabian, Polarimetric-spectral intensity modulation (P-SIM): enabling simultaneous hyperspectral and polarimetric imaging, in: Infrared Technology and Applications XXV, 1999, Orlando, FL, USA, p. 8.
[6] J. Craven-Jones, M.W. Kudenov, M.G. Stapelbroek, E.L. Dereniak, Infrared hyperspectral imaging polarimeter using birefringent prisms, Appl. Opt. 50 (8) (2011) 1170–1185.
[7] T. Mu, C. Zhang, C. Jia, W. Ren, Static hyperspectral imaging polarimeter for full linear stokes parameters, Opt. Express 20 (16) (2012) 18194–18201.
[8] X. Jian, C. Zhang, B. Zhao, Polarization detection with polarization interference imaging spectrometer, Optik – Int. J. For. Light. Electron. Opt. 122 (8) (2011) 677–680.
[9] K. OKA, T. KATO, Static Spectroscopic Ellipsometer Based on Optical Frequency-Domain Interferometry, Polarization Analysis, Measurement, and Remote Sensing IV, 2002, p.4.
[10] K. Oka, T. Kato, Spectroscopic polarimetry with a channeled spectrum, Opt. Lett. 24 (21) (1999) 1475–1477.

[11] T. Mu, C. Zhang, W. Ren, C. Jia, L. Zhang, Q. Li, Compact and static fourier transform imaging spectropolarimeters using birefringent elements, Int. Sympos. Photoelectron. Detect. Imag. Beijing (2013) 15 (cc).
[12] M.W. Kudenov, N.A. Hagen, E.L. Dereniak, G.R. Gerhart, Fourier transform channeled spectropolarimetry in the MWIR, Opt. Express 15 (20) (2007) 12792–12805.
[13] W. Xin-quan, X. Bin, H. Min, H.U. Liang, J. Juan-juan, Study and simulation of the intensity modulation-fourier transform spectropolarimeter, Spectrosc. Spect. Anal. 31 (7) (2011) 1980–1984.
[14] C. Zhang, Q. Li, T. Yan, T. Mu, Y. Wei, High throughput static channeled interference imaging spectropolarimeter based on a Savart polariscope, Opt. Express 24 (20) (2016) 23314.
[15] R.J. Bell, Introductory fourier transform spectroscopy, Am. J. Phys. 41 (1) (1972) 39–45.